Technical University of Denmark

DTU

Modeling the microstructural evolution during constrained sintering

Bjørk, Rasmus; Frandsen, Henrik Lund; Tikare, V.; Pryds, Nini

Publication date:
2012

Link back to DTU Orbit

DTU Library
Technical Information Center of Denmark

MODELING THE MICROSTRUCTURAL EVOLUTION DURING CONSTRAINED SINTERING

R. BJØRK[1], H. L. FRANDSEN[1], V. TIKARE[2], N. PRYDS[1]

[1] Department of Energy Conversion and Storage, Risø DTU Campus, Technical University of Denmark - DTU, Frederiksborgvej 399, DK-4000 Roskilde, Denmark

[2] Sandia National Laboratory, Albuquerque, New Mexico, USA

e-mail: rabj@dtu.dk

Abstract

A numerical model able to simulate solid state constrained sintering of a powder compact is presented. The model couples an existing kinetic Monte Carlo (kMC) model for free sintering with a finite element (FE) method for calculating stresses on a microstructural level. The microstructural response to the stress field as well as the FE calculation of the stress field from the microstructural evolution is discussed. The sintering behavior of two powder compacts constrained by a rigid substrate is simulated and compared to free sintering of the same samples. Constrained sintering result in a larger number of pores near the substrate as well as a reorientation of the pores along the direction normal to the substrate. These features are also observed experimentally.

1 Introduction

Many applications require components that are sintered under a variety of constraining stresses. These constraints may be internal such as those that arise during co-sintering of multiple layers densifying at different rates. Or the constraints may be external due to a rigid substrate constraining the densification of the adjacent surface or be due to an applied load.

A general review of constrained sintering, discussing both continuum and microstructural evolution, are presented in Reference [1]. Experimentally, samples sintering under constraints display anisotropic macroscopic shrinkage and porosity evolution. The overall change in size of a component sintering under constrains has been successfully modeled using different techniques. However, linking the macroscopic anisotropic shrinkage to anisotropy in the microstructure is difficult [1].

In this work, we present a model and apply it to study the microstructural evolution of a sample constrained during sintering on a rigid substrate, as this is a simplest example of constrained sintering. Constrained sintering of both porous gold and silver circuit film on a rigid substrate has been studied experimentally [2, 3]. The constrained films had higher porosity when compared to freely sintered films, but no change in grain size was observed. Tape cast and dip-coated alumina films sintered on a rigid substrate had pores perpendicular to the substrate surface and a higher porosity near the substrate [4, 5]. Elongated pores have also been observed for thin zirconia films sintered on rigid substrates [6]. Synchrotron computed microtomography has been used to study constrained viscous sintering of glass on a substrate [7], and several other studied on constrained viscous sintering of glass exist [8, 9, 10].

A numerical model that is able to simulate constrained solid state sintering and predict important microstructural properties, such as pore size and structure, would be of interest for a number of technological applications as macroscopic properties can depend directly on microstructural parameters [11]. A number of such models exist. The discrete element method (DEM) treats each grain as a spherical particle that interacts with neighboring particles by the Newtonian force laws. Densification is simulated by allowing the spheres to overlap, and therefore DEM is not able to simulate microstructural evolution, grain growth or late stage

sintering [12]. However, for early stage sintering, DEM models have replicated experimental observed trends, such as large and orientated pores near the substrate [12, 13]. Another approach used a surface-evolver program to calculate the equilibrium configuration of particles during constrained sintering [14, 15], but this approach is computationally intensive and cannot be used to model large complex microstructures.

We present a microstructure-scale model that can simulate the entire sintering process under constraining conditions. The model extends an existing kinetic Monte Carlo numerical model, which has previously been shown to correctly model the free sintering of copper spheres [16, 17], close-packed spheres [18] and powder compacts with a particle size distribution [19]. This model is coupled with a finite element model (FEM) to allow for the calculation of microstructural stresses during sintering. These local stresses are incorporated in the kMC model to simulate densification due to curvature and local stresses. Using a microstructural model to study constrained sintering is an ideal approach as powder compacts with the exact same microstructure can be sintered with and without constraints so that the results can be compared directly.

2 The kinetic Monte Carlo model of sintering

First, the stress-free kinetic Monte Carlo model used to model free solid state sintering is described. The model defines individual grains and pores on a two or three dimensional square/cubical grid, where a single grid cell is referred to as a voxel in both two and three dimensions. The model simulates grain growth, pore migration and vacancy formation and annihilation through diffusion processes. The driving force for sintering in the model is the capillarity (reduction of interfacial free energy), which is defined by the neighbor interaction energy between voxels.

The energy at a given site, i, is proportional to the sum of unlike neighbors to that site, i.e.

$$E_i = \frac{1}{2} \sum_{j=1}^{8 \text{ or } 26} J * (1 - \delta(q_i, q_j)) , \tag{1}$$

where J is the neighbor interaction energy, q_i and q_j are the state of the sites i and j respectively, and δ is the Kronecker delta function. A value of $J = 1$ is chosen, as this constitutes the simplest case possible. Grains are identified by different values of q, while all pore sites all have the same state, $q = 0$. The number of neighboring sites considered is 8 for a two dimensional simulation and 26 for a three dimensional one.

Sintering is modeled by interchanging two neighboring sites, altering the state of a single grain site or collapsing an isolated pore site, called a vacancy, by moving it to the surface of the sample. If any of these "moves" lowers the total energy of the system, as calculated by Eq. (1), then the move is accepted, whereas if the energy is increased the move may be accepted with probability P based on the standard Metropolis algorithm, defined as

$$P = \begin{cases} \exp\left(\frac{-\Delta E}{k_\text{B} T}\right) & \text{for } \Delta E > 0 \\ 1 & \text{for } \Delta E \leq 0 \end{cases} \tag{2}$$

where T is the temperature and k_B is Boltzmanns constant and where the different types of events can have different temperatures. The attempt frequency of each type of event can also be varied, allowing different magnitudes of pore surface diffusion, grain boundary diffusion and grain boundary mobility. The attempt frequency is the probability that a given type of move is attempted.

The kMC model conserves mass through sintering. However, the kMC model is inherently dimensionless and therefore both time, length and temperature in the model are in dimensionless units. Time is measured in Monte Carlo steps, MCS. One MCS has passed when the number of attempted grain growth moves equals the total number of grain sites in the system. Time measured in MCS and length are proportional to real units. The linear scaling can be determined by comparing the modeled system with a similar experimental system [16].

Under constrained sintering, the stresses present are an additional driving force for sintering and they modify the rates of the diffusive processes. The next section describes a coupled kMC-FE model for simulation of microstructural evolution during constrained sintering.

3 Including stress in the kinetic Monte Carlo model

To model constrained sintering, the evolution of the microstructure must depend on the local stresses in the sample. In the stress-free kMC model, sintering happens purely in response to the local environment, but when stresses are included in the model the microstructure must respond to events occurring further away in the sample. A finite element (FE) model has been implemented coupled to the existing kMC model to allow the stress to be calculated based on events that causes strain in the microstructure. The FE model is a purely elastic model. It allows for a direct calculation of the stress field in a sample based on the mechanical properties of the sample, i.e. Young's modulus and Poisson's ratio. The kMC model incorporates the stresses to simulate the differential densification in response to these stresses and the local curvatures. The FE model is written in C++ and the direct solution of the FE model is computed using Eigen v.3 [20].

Coupling a kMC model with a FE model for materials processes has previously been used for studying recrystallization in metals, where the FE model calculates deformation of a sample, while the Monte Carlo model simulate grain growth [21, 22, 23, 24]. Using voxel data obtained from e.g. a kMC sintering model, a method has also been developed that uses a finite element approach to determine e.g. tensile stress-strain curves [25]. A viscoplastic finite element continuum model, coupled with a Monte Carlo model for calculating microstructural strain rates have also been presented [26].

The aim of this manuscript is to present the general concepts of the coupled kMC-FE model and initial results. First, we discuss the microstructural response in the kMC model to a stress field, and subsequently how to calculate the stress field due to microstructural events using the FE model.

3.1 Coupling the microstructural evolution to the stress field

Suppose that the stress field is known throughout the microstructure at a given instant in time. The active processes during simple solid state sintering, i.e. grain growth, pore migration by surface diffusion, and vacancy generation, diffusion and annihilation are undoubtedly influenced by the stress, and thereby the microstructural evolution of the sample is altered.

Experiments on constrained sintering have shown that grain growth during sintering is not significantly affected by the stress field, and so grain growth in the model is not modified. In the current model, pore migration moves do not depend on the local pressure. The effect of stress on pore migration will be the topic of future work.

3.1.1 Annihilation events

Densification by annihilation is the principal process that leads to stress formation and deformation in the sintering powder compact. The annihilation event in the kMC model is therefore modified by altering the probability of annihilation due to the local stress state. Experimental observations indicate that compacts under compression densify more rapidly. To simulate this behavior the probability, P, defined in Eq. (2), is modified such that vacancy annihilation events depend on the local stress field, σ, through the expression

$$P = 0.5(1 - \tanh(\alpha p)) + 0.5, \tag{3}$$

This expression is then multiplied with the probability defined in Eq. (2). Here α is a constant and p is the local pressure, defined as $p = \sum_i^n \sigma_{ii}/n$, where $n = 2$ or 3 for two and three dimensional simulations, respectively. The constant α determines the strength of the coupling between the stress field and the microstructural evolution. In this model, vacancies under compressive load will be more likely to annihilate thus leading to higher densification rate, while regions under tension will densify more slowly or not at all. The annihilation path through the microstructure for a given annihilation event is not modified in the current model, but this will also be discussed in future publications.

The pressure is used in Eq. (3) as this is the first invariant of the stress field. More advanced models are also possible where, e.g. the stress in the direction of the annihilation path is used to calculate the probability instead of the pressure. Such model will be explored in a future publication.
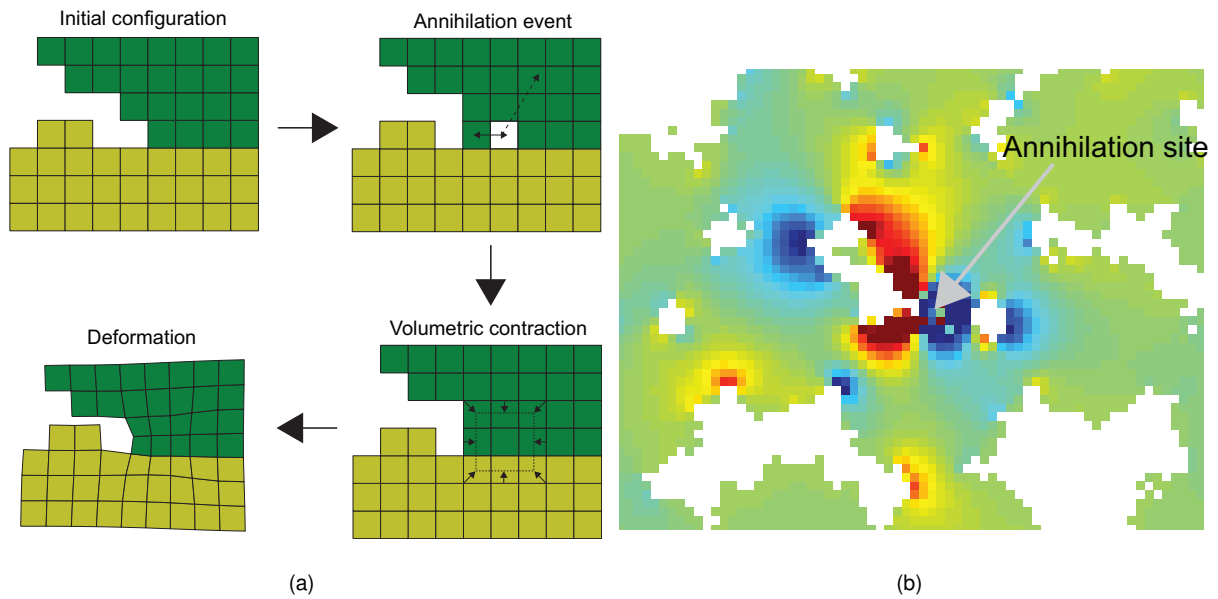
3

Figure 1: (a) An illustration of the stress generating process. A single vacancy site is generated at the grain boundary between two grains and annihilated. This corresponds to a volumetric strain, shown here in the surrounding sites, which causes a deformation of the microstructure. In the model the volumetric strain is applied in the center of mass of the grain. A surface plot of the resulting pressure, i.e. $1/2*(\sigma_{xx} + \sigma_{yy})$, is shown in (b). Here a red color indicates voxels under tension, while a blue color indicate compression.

3.2 Coupling the stress field calculation to the microstructural evolution

The stresses present during sintering are caused by the evolution of the microstructure due to differential densification at different locations in the powder compact or they can be due to an externally applied load. For the former case, the FE model uses annihilation events as the source of strain and calculates the stresses generated as a result. This is because in the kMC model densification is caused solely by the vacancy annihilation events. In such an event an isolated vacancy site is annihilated by collapsing a column of sites from the vacancy to the external surface of the sample into the vacancy. This process is in reality caused by the surrounding grain sites being redistributed to "fill" the vacancy. In the FE model this can be modeled by subjecting the surrounding sites to a volumetric strain, that causes a contraction in these sites that is large enough to fill the vacancy site.

In a real physical system the annihilation of the vacancies happen along the entire grain boundary. Therefore the volumetric strains in the FE model should be applied along the entire grain boundary where the annihilation event occurred. However, this is computationally unfeasible as all grain boundaries would have to be tracked throughout the simulation. Instead, the volumetric strain is applied in the center of mass of the adjacent particle. As the grains are typically small, the distance between the grain boundary and the center of mass of the adjacent grain is typically small, and thus this approach is justified. Applying the volumetric strain only at the annihilation site would make the local stress very high, preventing the microstructure from responding to far field stresses. The above described process of generating strain in the FE model is illustrated in Fig. 1. The applied volumetric strains causes a stress field that is computed using the FE model. The stress field calculated from the FE model from the annihilation event is also illustrated in Fig. 1.

The volumetric strains can be relaxed over time or be kept constant throughout the simulation time. For the systems studied here the strain is relaxed linearly to simulate viscous behavior as function of time, with an individual annihilation event being relaxed after 10000 MCS, corresponding to about 1% of the sintering time. The influence of this parameter on the microstructural

evolution will not be discussed in detail here.

The calculated stress field is linear in the chosen volumetric strain and the Youngs modulus chosen as input for the FE model. Therefore, the choice of volumetric strain and Youngs modulus only influence the value of the coupling constant, α, and therefore both have been chosen to equal one. Poisson's ratio is chosen to be 0.3, which is a typical value for most materials studied in sintering. Solving the FE model increases the total simulation time of about a factor of 5 for the two dimensional simulations considered here. A detailed investigation of the computation time has not been conducted yet.

The model presented here bear resemblance to the inelastic mechanical model introduced in Reference [28]. In this model changes in internal variables can cause a system to respond elastically. Here, the strains in the FE model do result from changes in internal variables of the system, namely the annihilation event occurring in the kMC microstructure. These annihilations can be viewed as inelastic or viscous deformations, which then cause the remaining system to respond elastically through the FE model.

3.3 Meshing the FE model

The stress must be calculated on at least the scale on which the microstructural evolution takes place, i.e. on the voxel scale. As sub-voxel resolution is not meaningful, the computational mesh for the FE model is chosen to resolve the microstructure at the voxel level. This is also a sufficient resolution as the FE model will not be used to capture surface stresses, as the energy due to surface tension is inherently modeled in the kMC model. In two dimensions a single voxel can either be meshed as two linear triangular elements or as one bilinear element. In three dimensions the choice is between five linear tetrahedral elements or one trilinear element. Regardless of choice, the number of nodes in the mesh remains the same, but the connectivity of the nodes is different. The simplest mesh is chosen, which is the bilinear and trilinear elements for the two- and three dimensional cases, respectively. Thus in the FE model each voxel in the kMC model corresponds to a single finite element. The pore sites, which are empty sites in the kMC model, are not meshed.

As the microstructure changes continuously, the stress should ideally be computed for every kMC step. However, this is not computationally possible, and instead the stress field is only computed after a MCS, where an annihilation event occured, which in practice is every few MCS. This results in a minimal difference in the stress field, as only pore migration moves have occurred in this time. After all annihilation events in an MCS have taken place the microstructure is remeshed completely. The annihilations that occurred in previous MCS are displaced to the new mesh based on the strain of the sample between the time that the event occurred and the current time.

3.4 A rigid substrate

When modeling sintering of a sample on a rigid substrate, the annihilation mechanism is modified further. For ordinary sintering, a vacancy annihilation event proceeds by moving voxels along a path between the annihilation site and the surface of the sample that passes through the center of mass of the grain involved in the annihilation event. When a substrate is present, annihilation paths that pass through or end at the surface of the substrate cannot be allowed. Therefore these annihilation paths are simply reversed, i.e. rotated 180 degree in the case of a two dimensional simulation. Furthermore the sample is assumed to be perfectly glued to the rigid substrate, and therefore pore migration moves are not allowed on the substrate surface. However, for non-perfect adhesion, pore migration could be made to depend on e.g. the local stress field and the friction coefficient between the sample and the substrate.

4 Model results

As discussed previously, a sample sintering constrained on a rigid substrate displays three characteristics; anisotropic shrinkage, more pores closer to the substrate and elongated pores perpendicular to the substrate. The goal of the work presented here is
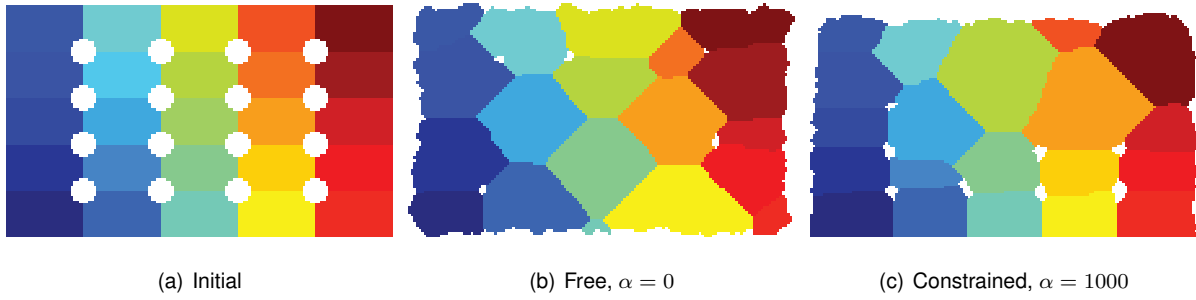
(a) Initial   (b) Free, $\alpha = 0$ (c) Constrained, $\alpha = 1000$

Figure 2: The initial microstructure (a) and the microstructure after 240000 MCS for a sample sintering freely with no stresses (b) and the same sample, constrained to a surface and with a strong coupling between the stress and the microstructure (c).

to investigate whether the model reproduce some of these features. The results of the modeling simulation will not be directly compared to an experimental data set, but the general validity of the model will be discussed.

Two types of powder compacts are studied; one with simple packing of monosized rectangular grains and a more realistic sample with randomly packed circular grains. Both are two dimensional. The latter sample geometry is generated by simulating the pouring of circular particles with diameters ranging between 13 and 19 voxels into a container. The numerical code used to simulate this behavior is the Large-scale Atomic/Molecular Massively Parallel Simulator (LAMMPS) code, available as open source from Sandia National Laboratories. The system with rectangular grains is a regular microstructure, similar to the one discussed in Reference [27]. This microstructure consists of rectangular grains with circular pores at the four grain boundaries. The grains are 30x18 voxels and the pores have a radius of 5 voxels.

For the modeling systems considered here the event temperatures are taken to be 0, 0.7 and 1 for grain growth, pore surface diffusion, and vacancy annihilation respectively. The attempt frequencies are taken to be 1, 1 and 5 for the same mechanisms, respectively. These values are chosen because they result in a realistic sintering behavior.

4.1 Powder compact of rectangular grains

Shown in Fig. 2 is the initial microstructure and the microstructure of a sample sintered freely and the same sample sintered on a rigid substrate with a strong coupling between the stress field and the microstructure, $\alpha = 1000$. The microstructure is shown after 240000 MCS. It can clearly be seen that the constrained sample has more pores near the substrate and the pore shape is elongated in the direction normal to the substrate. However, the statistics are small and the detailed pore shape and orientation have not been investigated yet. The stress field generated by the constraining surface implemented in the model, through the coupling between stress and microstructure, results in this behavior.

4.2 The randomly packed circular particle compact

A compact of randomly packed particles showed similar behavior when sintered on a rigid surface. Two different randomly packed compacts are considered; one with dimensions 200x200 voxels and one with 400x100 voxels.

For both the microstructural evolution is shown in Figs. 3 and 4. As with the rectangular grain system studied above, a strong coupling between stress and microstructure results in a more pores near the substrate, exactly as observed experimentally. The pores directly touching the substrate have a very slow rate of sintering, as pore migration is not allowed at the substrate surface. However, the inability of the pores in the lower part of the sample to sinter comes directly from the coupling between stress and microstructure. The same behavior is seen both for the 200x200 and the 400x100 system.

Studying the strain in the different directions to investigate if the samples display anisotropic shrinkage, as observed experimentally, will be presented in a future work.
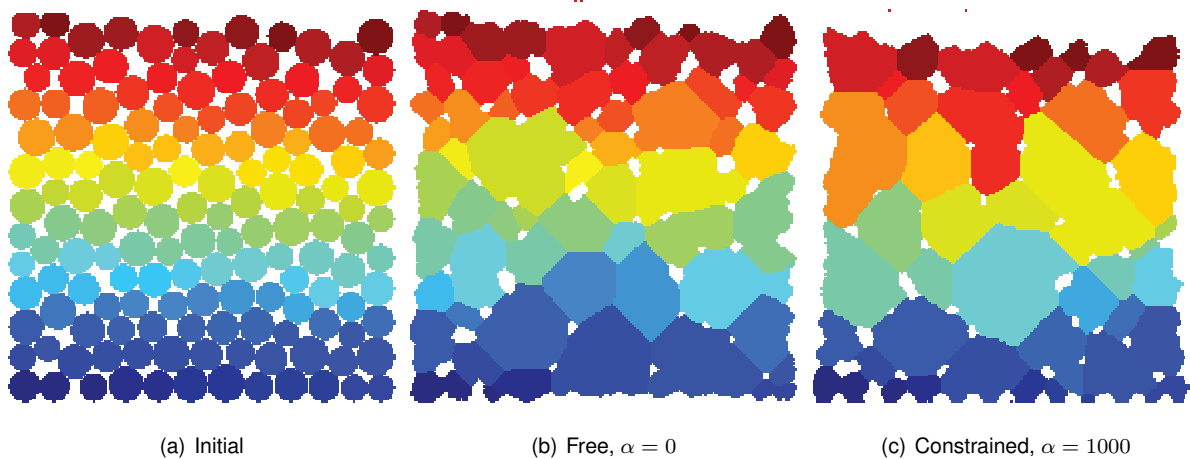
(a) Initial (b) Free, $\alpha = 0$ (c) Constrained, $\alpha = 1000$

Figure 3: The initial microstructure and the microstructure after 149000 MCS for a rectangular sample of random packed particles sintering freely with no stresses (a) and the same sample, constrained to a surface and with a strong coupling between the stress and the microstructure.
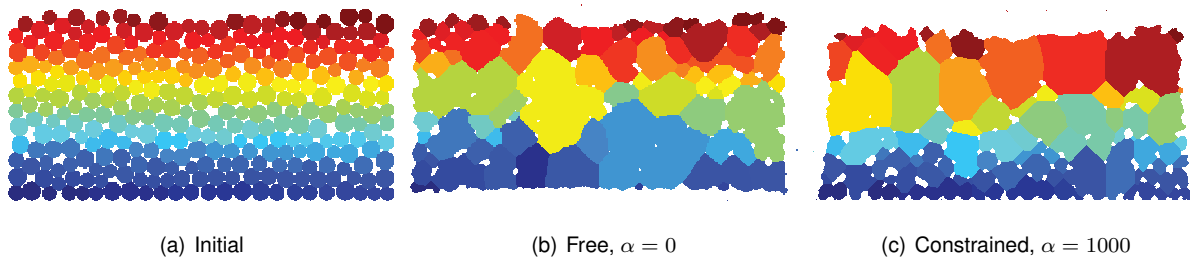

(a) Initial (b) Free, $\alpha = 0$ (c) Constrained, $\alpha = 1000$

Figure 4: The initial microstructure and the microstructure after 149002 MCS for an elongated sample of random packed particles sintering freely with no stresses (a) and the same sample, constrained to a surface and with a strong coupling between the stress and the microstructure.

5 Conclusion

A new microstructural model that couples a kMC sintering model and a finite element model for calculating stresses has been presented. The microstructural response to a stress field and the derivation of the stress field from the microstructural evolution was discussed. The sintering of two kinds of samples were modeled and the effect of the coupling between the stress field and the microstructure was explored. The response from the microstructure to the stress field was observed to lead to a larger number of pores near the substrate as well as a reorientation of the pores along the direction normal to the substrate, both features that are also observed experimentally.

Acknowledgements

References

[1] D. J. Green, O. Guillon, and J. Rödel, J. Europ. Ceram. Soc. 28 (2008) 1451-1466.

[2] J. W. Choe, J. N. Calata, and G.-Q. Lu, J. Mater. Res. 10 (1995) 986-994.

[3] Y.-C. Lin and J.-H. Jean, J. Am. Ceram. Soc. 87 (2004) 187-191.

[4] O. Guillon, S. Krauš, and J. Rödel, J. Europ. Ceram. Soc. 27 (2007) 2623-2627.

[5] O. Guillon, L. Weiler, and J. Rödel, J. Am. Ceram. Soc. 90 (2007) 1394-1400.

[6] R. Mücke, N. H. Menzler, H. P. Buchkremer, and D. Stoever, J. Am. Ceram. Soc. 92 (2009) 95-102.

[7] D. Bernard, O. Guillon, N. Combaret, and E. Plougonven, Acta Mater. 59 (2011) 6228-6238.

[8] J. N. Calata, A. Matthys, and G. Lu, J. Mater. Res. 13 (1998) 2334-2341.

[9] J. B. Ollagnier, D. J. Green, O. Guillon, and J. Rödel, J. Am. Ceram. Soc. 92 (2009) 2900-2906.

[10] J. B. Ollagnier, O. Guillon, and J. Rodel, J. Am. Ceram. Soc. 93 (2010) 74-81.

[11] Y. Boonyongmaneerat, Mater. Sci. Eng. A 452 (2007) 773-780.

[12] C. Martin and R. Bordia, Acta Mater. 57 (2009) 549-558.

[13] T. Rasp, A. Wonisch, T. Kraft, C. Jamin, and O. Guillon, J. Am. Ceram. Soc. 95 (2012) 586-592.

[14] F. Wakai and F. Aldinger, Acta Mater. 51 (2003) 641-652.

[15] F. Wakai and R. K. Bordia, J. Am. Ceram. Soc 95 (2012) 2389-2398.

[16] V. Tikare, M. Braginsky, D. Bouvard, and A. Vagnon, Comp. Mater. Sci. 48 (2010) 317-325.

[17] C. G. Cardona, V. Tikare, and S. J. Plimpton, Int. J. Comp. Mater. Sci. Surf. Eng. 4 (2011) 37-54.

[18] Bjørk, R., Tikare, V., Frandsen, H.L. and Pryds, N., Scripta Mater. 67 (2012) 81-84.

[19] Bjørk, R., Tikare, V., Frandsen, H. L. and Pryds, N., Submitted to J. Am. Ceram. Soc. (2012)

[20] G. Guennebaud, B. Jacob, *et al.*, "Eigen v3." http://eigen.tuxfamily.org (2010).

[21] G. Sarma, B. Radhakrishnan, and T. Zacharia, Oak Ridge National Laboratory Report (1996).

[22] B. Radhakrishnan, G. Sarma, and T. Zacharia, Oak Ridge National Laboratory Report (1998).

[23] D. Raabe and R. C. Becker, Model. Sim. Mater. Sci. Eng. 8 (2000) 445-462.

[24] L. Wang, X. Guan, B. Yu, X. Shen, Q. Zeng, and J. Zhao, Sec. Int. Conf. Intell. Comp. Tech. Autom. 2 (2009) 116-119.

[25] L. L. Mishnaevsky Jr., Mater. Sci. & Eng. A 407 (2005) 11-23.

[26] K. Mori, H. Matsubara, and N. Noguchi, Int. J. Mech. Sci., 46 (2004) 841-854.

[27] V. Tikare, M. Braginsky, E. Olevsky, and D. Lynn Johnson, J. Am. Ceram. Soc. 88 (2005) 59-65.

[28] J. Rice, J. Mech. Phys. Solids 19 (1971) 433-455.